

Reasonable Non-conventional Generator of Random Linear Chains Based on a Simple Self-avoiding Walking Process: A Statistical and Fractal Analysis

David R. Avellaneda B.[1], Ramón E. R. González[2(✉)], Carlos Andrés Collazos-Morales[3(✉)], and Paola Ariza-Colpas[4]

[1] Departamento de Estatística e Informática, Universidade Federal Rural de Pernambuco, Recife, Pernambuco CEP 52171-900, Brazil

[2] Departamento de Física, Universidade Federal Rural de Pernambuco, Recife, Pernambuco CEP 52171-900, Brazil
ramon.ramayo@ufrpe.br

[3] Vicerrectoria de Investigaciones, Universidad Manuela Beltrán, Bogotá, Colombia
carlos.collazos@docentes.umb.edu.co

[4] Departamento de Ciencias de la Computación y Electrónica, Universidad de la Costa, Barranquilla, Colombia

Abstract. Models based on self-excluded walks have been widely used to generate random linear chains. In this work, we present an algorithm capable of generating linear strings in two and three dimensions, in a simple and efficient way. The discrete growth process of the chains takes place in a finite time, in a network without pre-established boundary conditions and without the need to explore the entire configurational space. The computational processing time and the length of the strings depending on the number of trials $N^{'}$. This number is always less than the real number of steps in the chain, N. From the statistical analysis of the characteristic distances, the radius of gyration (R_g), and the end-to-end distance (R_{ee}), we make a morphological description of the chains and we study the dependence of this quantities on the number of steps, N. The universal critical exponent obtained are in very good agreement with previous values reported in literature. We also study fractal characteristics of the chains using two different methods, Box-Counting Dimension or Capacity Dimension and Correlation Dimension. The studies revealed essential differences between chains of different dimensions, for the two methods used, showing that three-dimensional chains are more correlated than two-dimensional chains.

Keywords: Self-avoiding random walk · Linear chains · Critical exponents · Fractal dimension · Radius of gyration · End-to-end distance

© Springer Nature Switzerland AG 2021
O. Gervasi et al. (Eds.): ICCSA 2021, LNCS 12949, pp. 192–206, 2021.
https://doi.org/10.1007/978-3-030-86653-2_14

1 Introduction

SAWs describes a large spectrum of real systems. One of the first theoretical approaches to this subject is Flory's theory [1]. This theory helped to understand the power laws characteristic of this model and the role of dimensionality, using mean field arguments involving the concept of excluded volume. Other analytical approaches that used rigorous approximate methods such as perturbation theory, self-consistent field theory, and renormalization group, produced estimates with a certain degree of precision for critical exponents and some universal amplitude ratios [2–4].

Numerical methods are an important tool in the study of the properties of long SAW's [5]. These numerical approaches allow us to find the number of possible SAWs of length N. Universal properties are estimated using different techniques such as the ratio method, Pade approximants, or differential approximants, having reported results for square and cubic networks up to $N = 71$ and $N = 21$ steps, respectively [2, 6, 7]. In a SAW of length N, there are $2 \times d$ options for the first step of the walk and at most, $2 \times d -$ 1choices for the rest of the $N - 1$ steps. The number of configurations for as specific value of $N(C_N)$, is in the range: $dN \leq C_N \leq (2d)(2d-1)^{N-1}$, causing this number to grow with N according to a power law of the type $C_N \sim N^{\gamma-1}$, where γ is an universal critical exponent that depends on network dimension [8–10].

In this work we will not take into account the high number of walks possible for a specific N, but we show that the exponents characteristic of this type of system can be obtained from a subset of all possible configurations. In this work we focus in studying relatively small SAW chain ensembles, which might be relevant in order to reproduce the main characteristics of random linear chains, such as universal critical exponents. It is understood that we are referring to classic SAWs, where the walker tends to take steps at random, avoiding regions of the space already visited by him. These are not self-repelling chains, for which all possible configurations for a given length are considered. In this last type of chain, it is associated with a statistical weight, represented by the Boltzmann factor, with a potential energy proportional to the number of self-intersections [11].

As a complement to the study, we implement a comprehensive analysis of the fractal dimension of the generated chains using two different methods: box-counting dimension and correlation dimension.

The main motivation of this work is to be able to generate sets, statistically representative, of linear chains with known universal characteristics and behaviors, without having to go through the entire configurational space. For a SAW of length N, there are 2d options for the first step of the walk and at least 2d-1 choices for the rest of the N-1 steps, this makes the value of the number of possible configurations (c_N) that a SAW of N steps can adopt, starting from the origin, grow with a power law. A huge effort has been made in the last 6 decades to develop efficient methods for counting SAWs, but knowing the exact values of CN and exponents still represents an open challenge. With our work, we show that only with a subset of all possible configurations we can obtain exponents similar to those reported in the literature.

The paper is organized as follows. In the next section, we briefly review the SAW and its main characteristics, the proposed algorithm, as well as the definitions of the characteristic distances and the methods that will be used in the calculation of the fractal dimension of the chains. The subsequent section is dedicated to the discussion of the results of our simulations and finally, we expose the conclusions of the work.

2 Methodology

The objective of this work is to efficiently generate sets of two- and three-dimensional linear chains, with the typical characteristics of this type of system. Each chain is generated from the path taken by a randomly moving particle within a network without boundary conditions, with the limitation that the particle cannot pass through places previously visited by it.

2.1 Numerical Algorithm

For a d–dimensional network with free boundaries the algorithm to generate a one chain is as follows:

1. Choose the number of attempts $N^{'}$.
2. Choose the origin of the polymer, which in our case is the origin of the coordinate system.
3. Generate the first step randomly or choose it arbitrarily from a point in the cubic network.
4. Choose the following step randomly from one of the $2 \times d$ possible steps.
5. If the given step leads to self-intersection, go to item 4 and try again with another step. This step is most important to ensure the SAW.
6. If the step leads to an available location, add the step to the walk.
7. If the number of attempts is reached or if the number of possible steps is zero (the walker gets stuck), the simulation is accepted and saved.

Thus, the random chain is formed by N steps generated from $N^{'}$ attempts, and the representative flowchart of this process is shown in the Fig. 1.

After generating the random chain, we store the positions of each of the sites that make up the chain and start computing the characteristic measurements of its configuration. First, we calculate the position r_i of each site to obtain the center of mass r_C, with which we obtain the radius of rotation, R_g. Next, we calculate the end-to-end vector module, R_{ee}, which can be easily derived from the distance of the *Nth* site to the origin of the chain. All these quantities are properly defined in the next subsection.

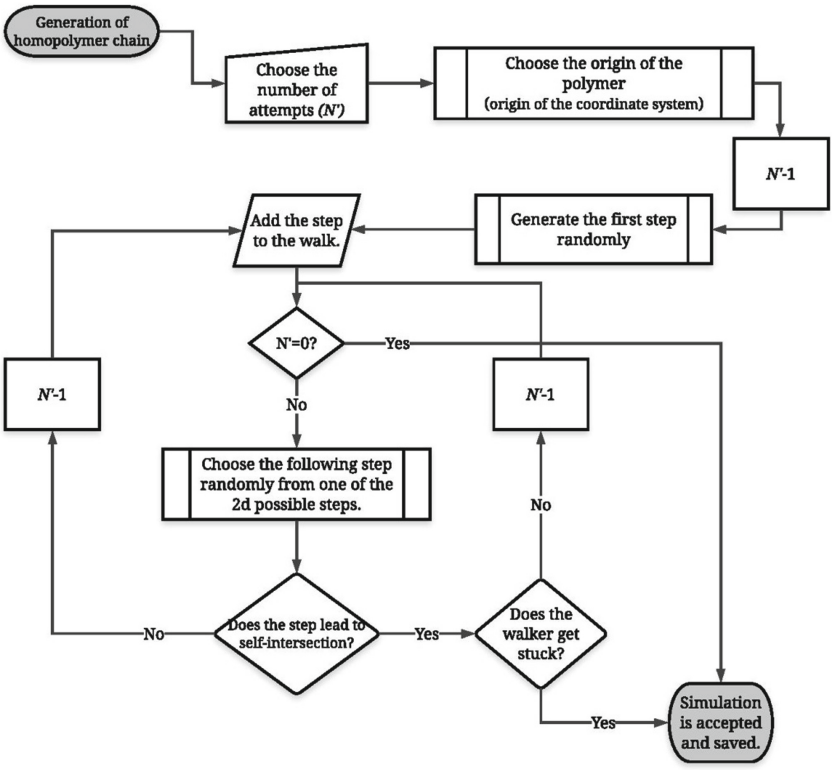


Fig. 1. Flowchart of the computational algorithm used to generate an isolated linear chain in a d-dimensional network.

2.2 Characteristic Distances and Flory Exponent

The proposed algorithm efficiently generates a set of linear chains in uniform $2D$ and $3D$ networks, each of them is formed by N sites in positions $\{r_0, r_1, ..., r_N\}$ in the space of dimension$d$. The separation distance between the site i and its nearest neighbour is $b = r_i - r_{i-1}$, for $i = 1, 2, ..., N$, which would be equivalent to a Kuhn segment [1, 12]. We describe the chain morphology by exploring the behavior of two characteristic distances, end-to-end distance R_{ee} and the radius of gyration R_g. The end-to-end distance is defined as the mean square variance of the displacement, and the radius of gyration represent the second moment around the center of mass. The expressions of these two quantities are shown below [12]:

$$R_{ee}{}^2 = \langle (r_N - r_0)^2 \rangle. \tag{1}$$

$$R_g^2 = \frac{1}{N+1} \sum_{i=0}^{N} \left\langle (r_i - r_C)^2 \right\rangle, \tag{2}$$

The variables r_N and r_0 are the positions of the end of a chain, and r_C is a centre of mass of the chain. For real chains, a relationship between these distances is [13]:

$$\frac{6{R_g}^2}{{R_{ee}}^2} = 0.952 \tag{3}$$

The dependence of the radius of gyration with N, size of a Kuhn segment b, and exponent γ, for this type of chain, responds to the expression below:

$$R_g = bN^{\nu} \tag{4}$$

The exponent γ is the Flory exponent [1, 12, 14], which comes from Flory's theory. Flory's exponent does not depend on the type of network, but on the spatial dimensionality d [10]. Generally, Flory's exponent is simply calculated from [14, 15]:

$$\nu = \frac{3}{d+2} \tag{5}$$

2.3 Fractal Dimension of Linear Chains. Box-Counting Dimension and Correlation Dimension

Self-similarity and self-affinity are important characteristics of linear chains. These properties are directly related to their configuration and that are well behaved for a defined variety of scales. Random linear chains in general can behave like random fractals [16–20]. The mean quadratic distance of the end-to-end vector is proportional to the number of connected segments (or Khun lengths), as shown in the following equation:

$$\langle {R_{ee}}^2 \rangle \sim N^{2\nu} \tag{6}$$

For any "r-size" subsection of the chain containing "n-sites", its characteristic size is equal to:

$$\langle r^2 \rangle \sim n^{2\nu} \Rightarrow r \sim bn^{\nu} \tag{7}$$

The degree of self-similarity for small scales is limited by the Kuhn length b, and the characteristic sizes, (R_g and R_{ee}) of the chain for large scales. Thus, the previous equation is valid for $b < r < R$. The fractal dimension suggests that the number of "segments" within a sphere of radius R is R^{d_F}, and since the behavior of R is known according to Flory's exponent, it is easy define the value of the fractal dimension according to the exponent ν given by [14, 18, 20, 21]:

$$d_F = \nu^{-1}. \tag{8}$$

The capacity dimension (box-counting dimension) is used to calculate the fractal dimension of binary images [16, 18, 19, 22–25]. Since it is a purely geometric method, it was only just used in two-dimensional chains. $2D$ images was generated, from the walks, considering that each "link" would fill the space between him and his closest

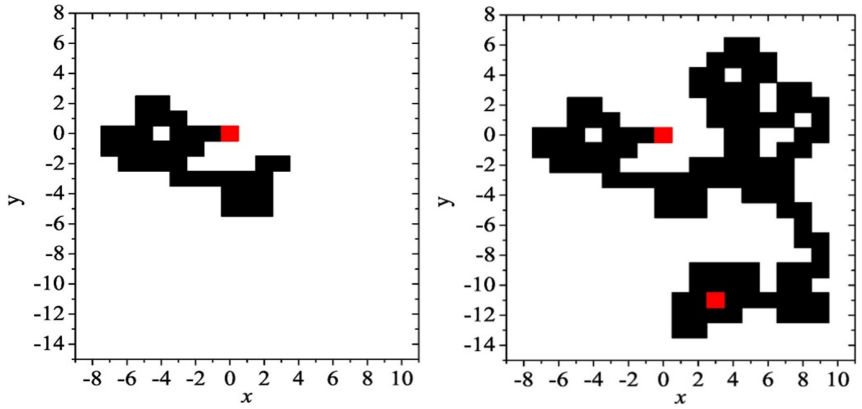


Fig. 2. Filling a path generated by a SAW of $N = 120$ that is born at the origin of the coordinate system. Two "moments" in the evolution of the walk is presented until it complies with the "stop" conditions established in the model.

neighbor, as we see in the Fig. 2. The correlation dimension, introduced in chaos theory [26, 27] is a measure of the dimensionality of the space occupied by an arbitrary set of points. In this case, the points are the positions of the steps of the random walks that generate the linear chains.

The correlation dimension was calculated from the time series of the Euclidean distance between the steps of the walk, both for two-dimensional chains and for three-dimensional chains. Although the strict definition of the d_F fractal dimension requires an "infinite scale reduction", this is not typical of real systems like our linear chains because their size is limited. Thus, $d_{F_{corr}}$ can only be measured within a scale range, which restricts the size of the strings. Because of this, chains with $N < 10$ were not considered in our calculations.

3 Results and Discussion

3.1 Algorithm and Simulations

In the algorithm each chain is generated from an initial number of attempts ($N^{'}$) that remain fixed during a set generation. Then, the random chain is formed by N "steps" generated from these $N^{'}$ attempts, so that, for a squared two-dimensional network, $N^{'} >> N$ and for a cubic three-dimensional network, $N^{'} > N$.

The different behaviors of N in function of $N^{'}$ for the two dimensions of networks respond to the fact that the chains can get trapped before reaching the total number of attempts. In the formation process of two-dimensional chains, there are a few degrees of freedom and the chains can be trapped more easily than in the case of three-dimensional chains.

There is no relationship between the number of attempts and the number of steps in this type of system. It was necessary to define an adequate number of attempts to construct a representative sample of linear chain states, guaranteeing, at the same time,

the optimization of the processing time of the computational code. We chose an interval between 2 and 2000 attempts, with a sequence of $N^{'}+2$ for the two-dimensional case and $N^{'}+5$ for the three dimensional. Within each interval, 10^4 simulations were performed for each $N^{'}$, thus generating 10^7 two-dimensional chains and 4×10^6 three-dimensional chains.

The results obtained in this system are illustrated in Fig. 3 in which two graphs are presented, one corresponding to the maximum number of steps and the other, to the processing time, both depending on the attempts. For the two-dimensional case (black points), the growth of the maximum number of steps (see Fig. 3a) is approximately linear until $N^{'} = 710$. From this point on, the maximum number of steps generated remains in an interval between $N = 366$ and $N = 690$ with a average value of $N \simeq 468$.

Concerning computational processing time (see Fig. 3b), we see a linear increase at a relatively low rate. For the three-dimensional case (grey diamonds), the maximum number of steps increases linearly (Fig. 3a) as the number of attempts increases. On the other hand, the computational processing time increases according to a power law as we can see in Fig. 3(b). These results were important in choosing a specific number of attempts to generate the chains according to their size, ensuring process efficiency as well as chains of various lengths, both large and small.

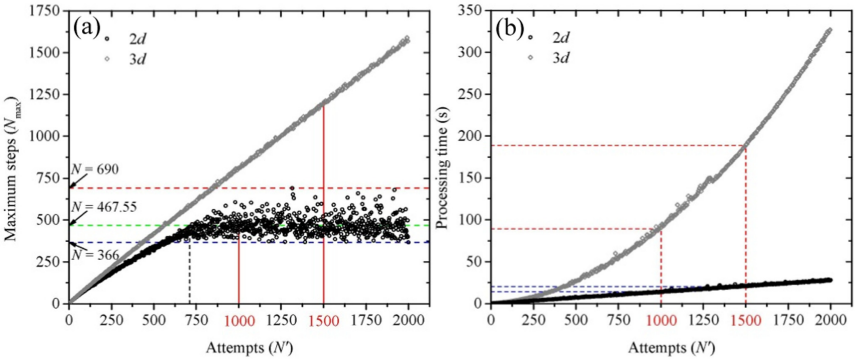


Fig. 3. Relationship between the number of steps N and the number of attempts $N^{'}$ for a sample of 10 thousand simulations in $2D$ and $3D$. Each point in Figure (a) represents the maximum size N_{max} of the series and (b) shows the processing time, in seconds, that it took to generate the 10 thousand simulations for each $N^{'}$.

We chose $N^{'} = 1000$ attempts for the two-dimensional case, since increasing this value would not benefit the generation of larger chains. For the three-dimensional case, an increase in $N^{'} \leftarrow$benefits the generation of larger chains, but would seriously compromise the processing time, for this reason, we use $N^{'} = 1500$.

3.2 Chain Length, Characteristic Distances and Flory Exponent

The distributions of the continuous variable Nb, that represents the length of a "fully stretched chain" with N "steps", for the generated sets of linear chains, are shown in Fig. 4.

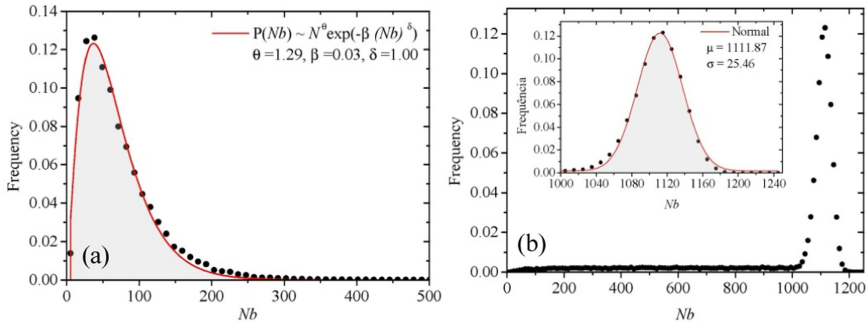


Fig. 4. Normalized histogram of the number of steps N for two-dimensional chains generated from $N^{'} = 1000$ attempts (a), and three-dimensional chains generated from $N^{'} = 1500$ attempts (b). The inset in (b) illustrates the histogram in a wide interval in which a Gaussian behavior occurs, with mean $\mu = 1111.87$ and standard deviation $\sigma = 25.46$.

For the bidimensional case, (Fig. 4a), the resulting curve is adjusted by a Fisher distribution. This curve presents an asymmetry, since the process of formation of two-dimensional chains is characteristic of a low number of degrees of freedom, generating, preferably, chains with small N. Three-dimensional chains (Fig. 4b), on the other hand, are much longer than two-dimensional. This behavior had already been explained previously. The process of forming chains in a three-dimensional network offers more possibilities of "escaping" to a site not yet visited, than in networks of two dimensions, where the probability of finding a "free" site is less, and the process can be interrupted more easily. For this reason, the vast majority are relatively large chains. For three-dimensional chains, the $Nb\psi$ values are uniformly distributed in the case of small chains, while very long chains have a normal distribution. The maximum of the distribution ($N = 1112$ steps for the chains generated from $N^{'} = 1500$), is obtained for large chains (compared to $N^{'}$). This way, chains with approximately this number of steps appear with greater probability under the conditions established in the simulation.

Figures 5 and 6, show the distribution of the characteristic distances (R_{ee} and R_g) of the chain. The graphs in Fig. 5 represent adjustments using Lhuillier's proposal [28]:

$$P(R) \sim exp\left(-R^{\alpha d} - R^{\delta}\right). \tag{9}$$

The distribution of characteristic distances, in Fig. 5, behaves according to two different exponential laws. The first exponential behavior in Eq. 8, corresponds to small values of characteristic distances, while the second term of this equation represents the behavior for large values. The α and δ exponents are associated with the universal exponent of Flory through the following expressions [29]:

$$\alpha = (\nu d - 1)^{-1}, \delta = (1 - \nu)^{-1} \tag{10}$$

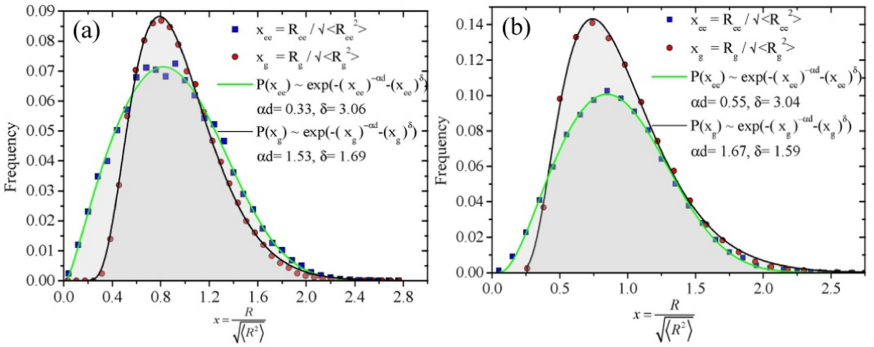


Fig. 5. Normalized histograms of the radius of gyration $R_g\,\psi$ and end-to-end distance R_{ee}. Behavior obtained for the ensemble of random chains generated from $N^{'} = 1000$ in $2D$ (a), and $N^{'} = 1500$ in $3D\psi$ (b). It is observed that a distributions agrees very well with the expression derived by Lhuillier [29, 30], both, the $R_g\,\psi$ and $R_{ee}\,\psi$ distribution.

Figure 6 shows the graphs of R_g and R_{ee} distribution, adjusted according to the Fisher-McKenzie-Moore-des-Cloiseaux law [12, 30–32]:

$$P(R) \sim R^{\theta} exp\left(-\beta R^{\delta}\right) \tag{11}$$

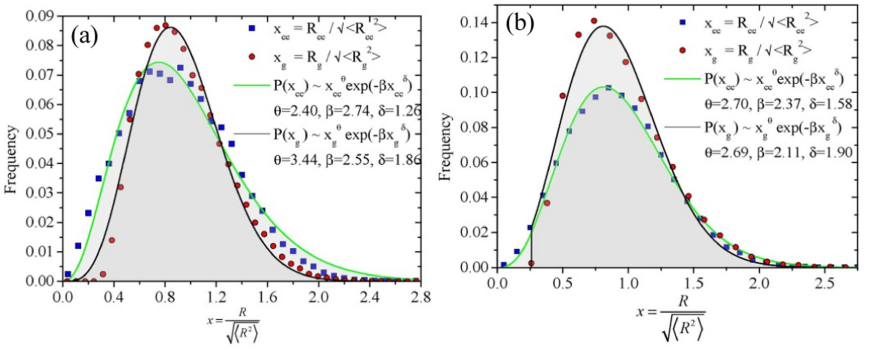


Fig. 6. Normalized histograms of the radius of gyration R_g and end-to-end discance R_{ee}. Behavior obtained for the ensemble of random chains generated from $N^{'} = 1000$ in $2D$ (a), and $N^{'} = 1500$ in $3D$ (b). It is observed that a distributions agrees very well with the function proposed by McKenzie and Moore [30] and des Cloizeaux [31, 32], both, the R_g and R_{ee} distribution.

The exponent θ characterizes the shorts-distance intra-chain correlations between two segments of a long chain.

$$\theta = (\gamma - 1)/\nu \tag{12}$$

The total number of a chain conformations is indirectly determined by the exponent γ. As opposed to ideal chains, where $\gamma = 1$, for real chains, $\gamma > 1$, i.e. there is a reduction of the probabilities in the distribution of R for short chains. The chains in this work were obtained from a random set without fixing the number of steps, unlike the theoretical distribution of Fisher-McKenzie-Moore-des-Cloiseaux [12, 31], although it is a different method to generate the chains, the characteristic distances follow the same distribution.

The value of Flory exponent ν, which describes the size of the linear chain, was calculated by computing the mean value of the radius of gyration (see Fig. 7). The values of ν obtained from the simulation, incorporated in the graphs, result closely approximate the expected theoretical value for the Flory exponent that is $\nu = 0.75$ and $\nu = 0.60$ for the two and three-dimensional case respectively. The calculation of ν of the behavior of R_g results in a value closer to the expected theoretical value than that calculated from the R_{ee}. The Flory exponent was also calculated indirectly from the δ exponent that results from the distribution of characteristic distances, shown in Figs. 5 and 6. The values of α and θ exponents were also obtained from these distributions, in indirect and direct ways, respectively.

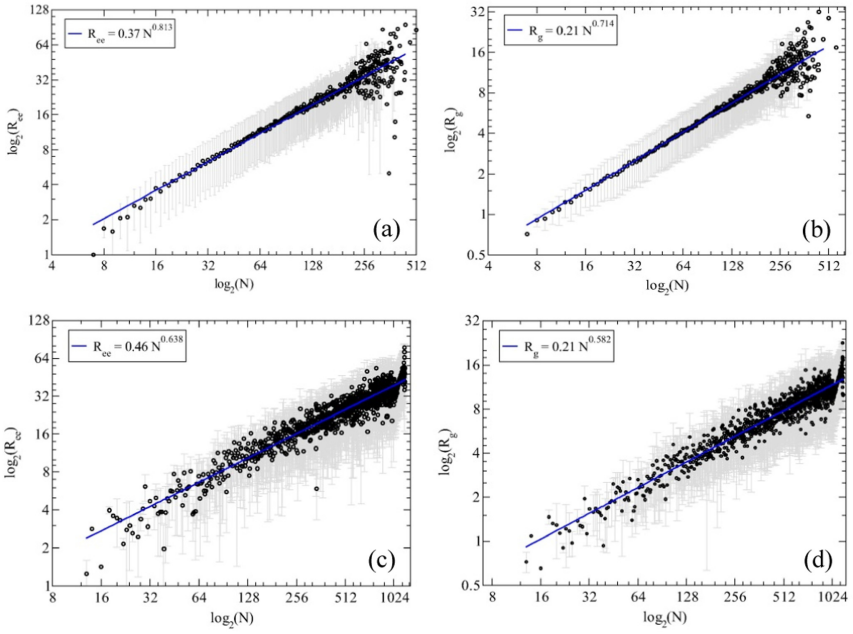


Fig. 7. Log-log scale representation of characteristic distances. Top panels, for 2D-chains: (a), the end-to-end distance (R_{ee}) as a function of the number of steps (N) with its respective value of $\nu = 0.757$; and (b), the radius of gyration (R_g) as a function of the number of steps (N) with its respective value of $\nu = 0.743$. Bottom panels, for 3D-chains: (c), the end-toend distance (R_{ee}) as a function of the number of steps (N) with its respective value of $\nu = 0.638$; and (d), the radius of gyration (R_g) as a function of the number of steps (N) with its respective value of $\nu = 0.582$.

Table 1 shows the values of exponents reported by our simulations. The above results have shown that although the two behaviors, R_{ee} and R_g, as a function of N fit a power law, the value of the characteristic exponent of R_g is closer to the theoretical value of Flory and to the values reported in [12, 33, 34]. Although, both proposed functions, fit well the distributions (R_{ee} and R_g), the values of the critical exponents obtained for each function, specifically the delta exponent, are different and correspond to different laws. The R_g distribution responds better to the law proposed by Lluillier, and the distribution of R_{ee}, to the Fisher-McKenzie-Moore-des Cloiseaux law.

Table 1. Main exponents calculated directly and indirectly from our simulations. The first and second rows show the exponents calculated from the behavior of the characteristic distances as a function of N. The exponents calculated using the distribution of R_{ee} and R_g appear in the next four rows. The exponents of the third and fourth rows were obtained using the Lhuillier distribution for both distributions. For the calculation of the exponents that appear in the last two rows, the Fisher-McKenzie-Moore-des-Cloiseuax (MMC) distribution was used.

Characteristic distances	$\nu(2D/3D)$	$\delta(2D/3D)$	$\alpha(2D/3D)$	θ
R_{ee} (vs. N)	0.81/0.64	5.26/2.76	1.61/1.09	–
R_g (vs. N)	0.71/0.58	3.45/2.39	2.38/1.34	–
R_{ee} (Lhuillier)	2.15	3.04	0.18	–
R_g (Lhuillier)	0.93	1.59	0.56	–
R_{ee} (MMC)	0.36	1.58	–	2.70
R_g (MMC)	0.47	1.90	–	2.69

Unlike our model, the previous models reported in the literature, simulate the growth of the chains keeping the N fixed. The parameters, despite being related to a universal growth exponent (Flory exponent), depend strongly of the system; as a result, obtained exponents in our simulations differ from those reported. The most important of these results is the form adopted by the distributions. We studied the distribution for a whole set of fifty thousand two and three-dimensional chains that are distributed as expected, with their own exponents and a positive asymmetry.

3.3 Fractal Dimension

The graphs in Fig. 8 show the results obtained regarding the analysis of the fractal dimension of the two and three-dimensional chains. The histograms reveal that, for the two-dimensional chains (Fig. 8a), the fractal dimension has a normal (Gaussian) behavior for the two method used, box-counting ($d_{F_{Box}}$) and correlation ($d_{F_{Corr}}$). Using the box-counting method (blue dots), the fractal dimension turned out to be less than the spatial dimension d and greater than the correlation dimension (red dots) whose averages were recorded in $\mu_{Box} = 1.698$ and $\mu_{Corr} = 1.189$. In this way, the inequality $d > d_{F_{Box}} > d_{F_{Corr}}$, is valid for our chains, as suggested by fractal theory [22]. Still, for the two-dimensional case, a peak corresponding to $d_{F_{Corr}}$ is closer to the theoretical value

of $d_{F_{2D}} = 1.33$. In the tree-dimensional case (Fig. 8b), the distribution of $d_{F_{Corr}}$ shows three peaks, in $d_{F_{1Corr}} \approx 1.45$, $d_{F_{2Corr}} \approx 1.64$ and $d_{F_{3Corr}} \approx 1.86$, with $d_{F_{2Corr}}$ being the most frequent value. In this case, the highest peak in the distribution approach the theoretical value of $d_{F_{3D}} = 1.7$. The quantitative results show that the values obtained from the correlation method are closer to the theoretical ones. On the other hand, the qualitative results reveal more information about the chains. The existence of three peaks reveals that three types of three-dimensional chains are formed during the growth process.

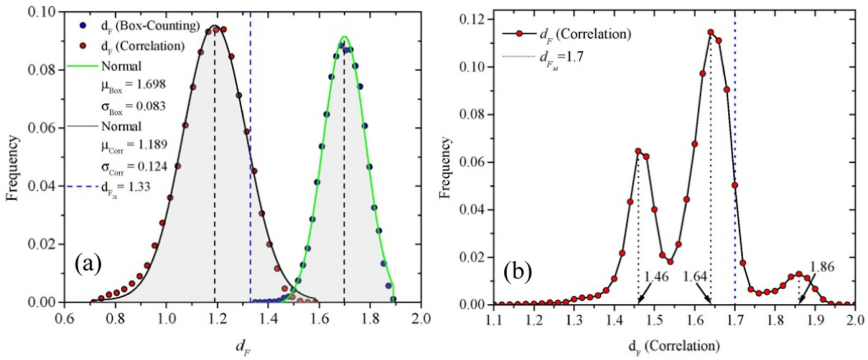


Fig. 8. Frequency distribution of the fractal dimension d_F obtained using the methods of box-counting, $d_{F_{Box}}$ (blue dots), for (a) the two-dimensional case and through the dimension of correlation, $d_{F_{Corr}}$ (red dots), for both (a) two-dimensional and (b) three-dimensional chains. The dashed black lines indicate the maximums obtained in each distribution, in the two-dimensional case it corresponds to the average values of the normal distribution (μ_{Box} and μ_{Corr}). The blue dashed lines represent the theoretical value of d_F which in (a) two-dimensional case is $d_{F_{2D}} = 1.33$ and, (b) three-dimensional is $d_{F_{3D}} = 1.7$. (Color figure online)

Figure 9 show the behavior of fractal dimension as a function of the number of steps, for 2D and 3D chains. Two-dimensional small chains have a high $d_{F_{Box}}$ dimension (Fig. 9a), this is because chains with a small number of steps can fill a large part of the space, which can be interpreted as well-compacted chains. As N increases, it is observed that the dimension $d_{F_{Box}}$ decreases, and for chains greater than $N = 200$, it remains within a region (dashed lines in Fig. 9a) oscillating around $d_{F_{Box}} = 1.587$.

The $d_{F_{Corr}}$ concerns the distribution of "links" within the chain structure. Figure 9, b and c, shows how as N grows, the correlation of the chains increases, but above a certain size ($N = 150$ for two-dimensional chains and $N = 500$ for three-dimensional), $d_{F_{Corr}}$ oscillates around specific average values, $d_{F_{Corr}} = 1.287$ and $d_{F_{Corr}} = 1.590$ for 2D and 3 D case respectively. In a "very" large N region, the correlation between chain "links" decreases uniformly, due to the fact that large chains have a much-stretched structure compared to smaller chains.

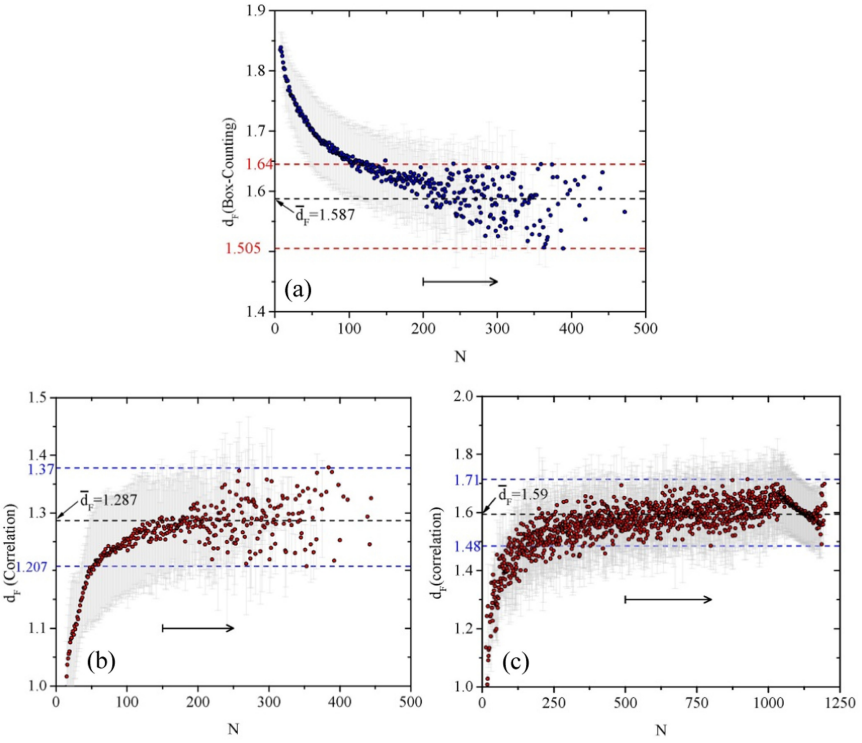


Fig. 9. Fractal dimension via *Box-Counting* ($d_{F_{Box}}$) (a), and via *correlation dimension* ($d_{F_{Corr}}$) (b and c) as a function of the number of steps (N) for two and three-dimensional chains. After reaching a size of $N \approx 200$, the fractal dimension stabilizes, oscillating around the value $d_F = 1.587$, in $2D$ case. In (b), when the strings reach a size of $N \approx 150$ the correlation dimension oscillates around $d_F = 1.287$. In (c), the dimension oscillates around $d_F = 1.59$ when the strings reach a size $N \approx 500$.

4 Conclusions

In this work, we show an algorithm based on natural self-avoiding random walk in square and cubic networks with no boundary was used to generate linear chains. The implementation of this algorithm is simpler and the computational cost is significantly lower than other approaches generally used to generate random linear chains. Although our method does not consider all possible configurations for the N size of the chain the values of the characteristic critical exponent's obtained by us are similar to those reported in the literature.

The study of the number of attempts (N') as a function of N, for two and three dimensions, showed that there are upper limits for N', above which there is no guarantee of better efficiency of the algorithm. This resulted in the optimization of the processing time in the construction of the set of chains. The exponents revealed by the power laws that govern these systems and the distribution of the characteristic magnitudes provides a solid basis for the study of linear chains in square and cubic networks.

The distribution of the characteristic distances for the linear chains obtained from our simulation shows a reasonable correspondence with that reported in the literature. Specifically, we prove that although it is possible to fit the two distributions ($R_g\psi$ and R_{ee}) using both Lhuillier's theory and the law proposed by FisherMcKenzie-Moore-des Cloiseaux, the obtained values of critical exponents such as ψ, ψ, $\psi\psi$ show us that the distribution of $R_g\psi$ responds better to the theory of Lhuillier, while in the case of the distribution of R_{ee}, the best fit is obtained with the Fisher-McKenzie-Moore-des Cloizeaux function. These results are in full agreement with the literature and reinforce the validity of the algorithm used when characterizing this type of system.

Both R_{ee} and R_g resulted in power functions of N and the values of the Flory exponent, in both cases, are quite close to the theoretical value, especially the value corresponding to R_g, showing that this characteristic distance is more appropriate when characterizing structurally this type of chains. Our model does not distinguish between chains of different sizes, showing that structural factors of the chains are invariant of scale. We also show that small chains are more correlated and, consequently, less flexible.

The fractal dimension of the two-dimensional chains is normally distributed, showing that the dimension by Box-counting is greater than the correlation dimension and both, smaller than the spatial dimension, as shown by the theory. In a three-dimensional case, the higher peak in the fractal dimension distribution is very close to the theoretical value. Finally, in very large three-dimensional chains the correlation decreases. This behavior can be associated with a change in the shape of the chains, which can form clusters separated by stretched structures. A more detailed analysis of the results and conclusions can be found in [35].

References

1. Flory, P.J.: Principles of Polymer Chemistry. Cornell University Press, Ithaca (1953)
2. Madras, N., Slade, G.: The Self-Avoiding Walk. Birkhauser, Basel (1953)
3. Yamakawa, H.: Modern Theory of Polymer Solutions. Harper and Row, New York (1971)
4. Wilson, K.G., Kogut, J.: The renormalization group and the expansion. Phys. Rep. **12**(2), 75–199 (1974)
5. Sokal, A.D.: Molecular Dynamics Simulations in Polymer Sciences. Oxford University Press, New York (1995)
6. Guttmann, A.J., Conway, A.R.: Square lattice self-avoiding walks and polygons. Ann. Comb. **5**(3), 319–345 (2001)
7. Jensen, I.: Enumeration of self-avoiding walks on the square lattice. J. Phys. A Math. Gen. **37**(21), 5503–5524 (2004)
8. Li, B., Neal, M, Sokal, A.D.: Critical exponent hyper scaling, and universal amplitude ratios for two and three-dimensional self-avoiding walks. J. Stat. Phys. **80**(3), 661–754 (1995)
9. Hara, T., Slade, G., Sokal, A.D.: New lower bounds on the self-avoiding walk connective constant. J. Stat. Phys. **72**(3), 479–517 (1993)
10. Slade, G.: Self-avoiding walk, spin systems and renormalization. Proc. R. Soc. A **475**(2221), 20180549 (2019)
11. Amit, D.J., Parisi, G., Paliti, L.: Asymptotic behavior of the "true" self-avoiding walk. Phys. Rev. B **27**(3), 1635–1645 (1983)
12. Rubinstein, M., Colby, R.H.: Polymer Physics. Oxford University Press, New York (2003)

13. Teraoka, I.: Polymer Solutions: An Introduction to Physical Properties. Wiley Inter-science, New York (2002)
14. Bhattarcharjee, S.M., Giacometti, A., Maritan, A.: Flory theory for polymers. J. Phys. Condens. Matter **25**, 503101 (2013)
15. Isaacson, J., Lubensky, T.C.: Flory exponent for generalized polymer problems. J. Phys. Lett. **41**(19), 469–471 (1980)
16. Mandelbrot, B.B.: The Fractal Geometry of Nature. W. H. Freeman and company, New York (1982)
17. Banerji, A., Ghosh, I.: Fractal symmetry of proteins interior: what have we learned. Cell. Mol. Life Sci. **68**(16), 2711–2737 (2011)
18. Dewey, T.G.: Fractals in Molecular Biophysics. Oxford University Press, New York (1997)
19. Maritan, A.: Random walk and the ideal chain problem on self-similar structures. Phys. Rev. Lett. **62**(24), 2845–2848 (1989)
20. Kawakatsu, T.: Statistical Physics of Polymers: An Introduction. Springer-Verlag, Heidelberg (2004)
21. Rammal, R., Toulouse, G., Vannimenus, J.: Self-avoiding walks on fractal spaces: exact results and Flory approximation. J. Phys. **45**(3), 389–394 (1984)
22. Takayasu, H.: Fractals in the Physical Sciences. Manchester University Press, New York (1990)
23. Feder, J.: Fractals. Physics of Solids and Liquids. Springer-US, New York (1988)
24. Theiler, J.: Estimating fractal dimension. J. Opt. Soc. Am. A **7**(6), 1055–1073 (1990)
25. Nayfeh, A., Balachandran, B.: Applied Nonlinear Dynamics: Analytical, Computational, and Experimental Methods. Wiley Series in Nonlinear Sciences, Germany (2008)
26. Grassberger, P., Procaccia, I.: Characterization of strange attractors. Phys. Rev. Lett. **50**, 346–349 (1983)
27. Grassberger, P., Procaccia, I.: Measuring the strangeness of strange attractors. Phys. D Nonlin. Phenom. **9**(1), 189–208 (1983)
28. Lhuillier, D.: A simple model for polymeric fractals in a good solvent and an improved version of the Flory approximation. J. Phys. Fr. **49**(5), 705–710 (1988)
29. Victor, J.M., Lhuillier, D.: The gyration radius distribution of two-dimensional polymers chains in a good solvent. J. Chem. Phys. **92**(2), 1362–1364 (1990)
30. McKenzie, D.S., Moore, M.A.: Shape of self-avoiding walk or polymer chain. J. Phys. A Gen. Phys. **4**(5), L82–L85 (1971)
31. des Cloizeaux, J.: Lagrangian theory for self-avoiding random chain. Phys. Rev. A. **10**, 1665 (1974)
32. des Cloizeaux, J., Jannink, G.: Polymers in solution: their modelling and structure. Oxford Science Publications. Clarendon Press, Oxford (1990)
33. Caracciolo, S., Causo, M.S., Pelissetto, A.: End-to-end distribution function for dilute polymers. J. Chem. Phys. **112**(17), 7693–7710 (2000)
34. Vettorel, T., Besold, G., Kremer, K.: Fluctuating soft-sphere approach to coarse-graining of polymer models. Soft Matter **6**, 2282–2292 (2010)
35. Bernal, D.R.: PhD Thesis, http://www.ppgbea.ufrpe.br/sites/www.ppgbea.ufrpe.br/files/documentos/tese_david_roberto_bernal.pdf. Accessed 21 June 2021